not only in biological systems and chemical processes, but also in the creation of molecular devices.

After this manuscript had been submitted, Isnin and Kaifer[13] reported the synthesis of a zwitterionic rotaxane containing a single cyclodextrin molecule. □

Received 9 September 1991; accepted 12 February 1992.

1. Lehn, J.-M. *Angew. Chem. Int. Ed. Engl.* **29,** 1304–1319 (1990).
2. Agam, G., Graiver, D. & Zilkha, A. *J. Am. chem. Soc.* **98,** 5206–5216 (1975).
3. Agam, G. & Zilkha, A. *J. Am. chem. Soc.* **98,** 5214–5216 (1976).
4. Ogino, H. *J. Am. chem. Soc.* **103,** 1303–1304 (1981).
5. Ogino, H. & Ohata, K. *Inorg. Chem.* **23,** 3312–3316 (1984).
6. Gibson, H. W. *et al. Makromolec. Chem., Makromolec. Symp.* **42/43,** 395 (Hüthig & Werf, Basel, 1991).
7. Ashton, P. R. *et al. Angew. Chem. Int. Ed. Engl.* **30,** 1042–1045 (1991).
8. Manka, J. S. & Lawrence, D. S. *J. Am. chem. Soc.* **12,** 2440–2442 (1990).
9. Rao, T. V. S. & Lawrence, D. S. *J. Am. chem. Soc.* **112,** 3614–3615 (1990).
10. Harada, A. & Kamachi, M. *Macromolecules* **23,** 2821–2823 (1990).
11. Harada, A. & Kamachi, M. *J. chem. Soc., Chem. Commun.* 1322–1323 (1990).
12. Bergeron, R. J., Channing, M. A., Gibeily, G. J. & Pillor, D. M. *J. Am. chem. Soc.* **99,** 5146–5151 (1977).
13. Isnin, R., Kaifer, A. E. *J. Am. chem. Soc.* **113,** 8188–8190 (1991).

Imaging the ocean with ambient noise

Michael J. Buckingham*†, Broderick V. Berkhout* & Stewart A. L. Glegg‡

* Marine Physical Laboratory, Scripps Institution of Oceanography, La Jolla, California 92093-0213, USA
‡ Department of Ocean Engineering, Florida Atlantic University, Boca Raton, Florida 33431, USA

FOR many years, the principal means of probing the ocean using sound has been through the use of 'active' or 'passive' techniques. With an active system, an object is illuminated by a pulse of sound and its presence inferred from the echo it produces, whereas the passive approach involves simply listening for the sound that the object itself emits. Here we report a new method of using sound in the ocean, which is neither passive nor active. It relies on the naturally occurring, incoherent ambient noise field in the ocean—which can be thought of as 'acoustic daylight'—as the sole source of acoustic illumination. By focusing the sound scattered by an object immersed in the noise field, it should be possible to produce a visual image of the object on a television monitor. We have tested this concept by conducting a simple experiment in the ocean, with a parabolic reflector acting as an acoustic lens, and our results confirm that objects illuminated only by ambient noise can indeed be 'seen' at frequencies between 5 and 50 kHz.

The ocean is an acoustically noisy environment[1]. Sources of the ambient noise field include a variety of natural mechanisms[2], many of which are associated with breaking surface waves[3] and other surface phenomena. Over the frequency range between 1 and 50 kHz, the power spectral density of sea-surface noise shows a negative gradient, varying with frequency f as f^{-n}, where $n \approx 2$. Surface-generated noise takes the form of an incoherent, propagating radiation field, with energy travelling in all directions, and in this sense is analogous to daylight in the atmosphere. Above 50 kHz or so, depending on sea state, thermal noise arising from brownian motion of the water molecules dominates the ambient noise spectrum[4]. Thermal noise is a localized, non-radiating, microscopic phenomenon, which shows a spectrum with positive gradient, varying with frequency as f^2. Figure 1 illustrates both the radiating, surface-generated noise and the thermal noise components of the ambient noise spectrum.

Recent experiments[5] have shown that geo-acoustic information about the ocean environment can be extracted from the ambient noise. Here we report the use of ambient noise to form pictorial images of objects in the ocean. We can draw an analogy between the natural optical (daylight) field in the atmosphere and the radiating ambient noise in the ocean: both fields consist of random, incoherent radiation propagating in all directions. For this reason the concept of imaging with ambient noise, which was proposed by one of us (M.J.B.) several years ago, has been designated 'acoustic daylight'.

An object in the ambient noise field modifies the field by scattering acoustic energy in all directions. This scattered radiation can be focused onto an image plane by an acoustic lens (which could be an acoustic refractor, reflector or phased array), allowing, after appropriate signal processing, a pictorial image of the object to be displayed on a television monitor. In principle, the screen image could move and could have computer-constructed colour, corresponding to the 'acoustic colour' (the frequency-dependent acoustic albedo) of the object space. In effect, the acoustic daylight scheme consists of an acoustic 'video camera', which relies on illumination from the natural sound field in the ocean to produce the final picture.

Although the analogy between daylight and ambient noise provides a useful introduction to the concept of acoustic daylight, it obviously cannot be pursued too far. For instance, the acoustic wavelength in the ocean at a frequency of 50 kHz is 3 cm, compared with 5×10^{-5} cm for the wavelength of green light in the atmosphere. The pupil of the human eye is ~20,000 optical wavelengths in diameter, which accounts for the excellent angular resolution of human vision. To achieve similar resolution with an acoustic lens working at 50 kHz would require an aperture of 600 m. Practical considerations dictate that a much smaller aperture be used in practice, yielding a corresponding reduction in angular resolution. Nevertheless, satisfactory images could still be obtained, especially if image enhancement techniques similar to those developed for synthetic-aperture radar and infrared remote sensing imagery were applied.

Another factor that will limit the performance of an acoustic daylight imaging system is sound absorption in the ocean. At 20 kHz the volume attenuation is ~3 dB km^{-1} (ref. 1), suggesting that the range achievable with the system is likely to be less than 1 km, although an improvement could be obtained by working at lower frequencies provided the reduction in angular resolution could be tolerated. For the moment, a reasonable operating frequency range for the acoustic daylight system is taken to be 5–50 kHz, with the lower limit set (rather arbitrarily) by angular resolution considerations and the upper limit determined by the onset of thermal noise (Fig. 1). As thermal noise is molecular in origin, it contains no information about the object and hence cannot be used for imaging.

Imaging with incoherent, natural sound is distinct from both

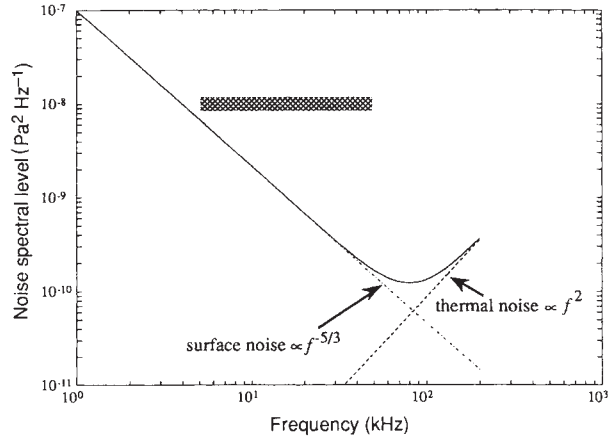

FIG. 1 Nominal ambient noise spectrum (solid line) in the ocean. The cross-hatched bar depicts the frequency range of interest in the acoustic daylight imaging experiment.

† Also at the Institute of Sound and Vibration Research, The University, Southampton SO9 5NH, UK.

passive and active detection, which are the conventional acoustic methods used to probe the ocean. Potentially, the new technique offers several advantages. As it does not require the transmission of acoustic energy (unlike active systems), it is attractive in connection with submarine operations. For example, mounted on the bow of a submarine, an acoustic daylight 'camera' could act as an aid to navigation by providing forward vision, a facility which would be particularly useful under the Arctic ice cap, where ice keels may protrude 40 m or more below the surface. Acoustic daylight might also be useful for undersea detection, as quiet or silent objects, which are undetectable by passive systems, are visible with the incoherent imaging technique.

Other possible uses include subsurface monitoring of oil rigs, surveillance of harbour entrances and bottom surveying, all of which would benefit from the fact that no sound transmission is required. A further desirable feature of the technique is that 'unwanted' noise sources, including reverberation and multipath, which degrade active and passive system performance, actually enhance the acoustic daylight image by providing better acoustic illumination. And perhaps it is worth emphasizing that the final acoustic-daylight display would be a pictorial image on a screen, unlike the outputs of active and passive systems, which can be interpreted only by trained operators.

To test the acoustic daylight concept, we recently did a simple experiment off the end of Scripps pier in which a parabolic reflector of diameter 1.22 m, with a neoprene rubber, pressure-release surface, was used as the acoustic lens. A low-noise hydrophone, shielded at the rear to block direct radiation, was mounted at the focus of the parabolic dish. The water depth at the end of the pier is ~7 m, and the weather conditions during the 3-day experiment were calm (sea-state 1 or less).

Three rectangular targets, consisting of thick plywood board with neoprene rubber facing, were the objects to be 'imaged'. The targets were placed in the main lobe of the reflector, either broadside-on (the 'on' position) or edge-on (the 'off' position) to the parabolic dish. Two orientations of the beam were tried: obliquely seaward, as illustrated in Fig. 2, and obliquely shoreward. As the results obtained with the seaward and shoreward configurations are qualitatively similar, only the former are reported here.

The three targets, each of which is 0.9 m high and 0.77 m wide, were placed ~7 m from the reflector. With this arrangement, the total target width was the same as the width of the main lobe of the reflector, as measured at the −6 dB points, at a frequency of 9 kHz. Throughout most of the 5–50 kHz frequency band of interest, therefore, the targets filled the beam. Noise spectra taken over the frequency range 5–50 kHz for the seaward orientation of the beam are shown in Fig. 3*a*. Both spectra are averages of several hundred spectra obtained from time-series data falling within a window of 2 s duration. The spectral resolution is 100 Hz.

The solid line in Fig. 3*a* represents the noise level with the targets 'on' and the broken line with the targets 'off'. The noise level across the band is ~4 dB higher when the targets are 'on' than when they are 'off'. Such behaviour was observed consistently throughout the duration of the experiment, and it is also consistent with the results of analogous experiments[6] conducted in air, in a hard-walled laboratory, with sound fields generated by loudspeakers. Figure 3*b*, showing the difference between the 'on' and 'off' spectra in Fig. 3*a*, indicates clearly that we can 'see' the targets when they are illuminated solely by the natural ambient noise field in the ocean.

The observed difference signal of nominally 4 dB is believed to occur because the noise around Scripps pier shows some horizontal directionality, being generated largely by the pier itself. (The pilings of the pier are encrusted with molluscs, and passing waves create an audible signal in the atmosphere.) Our experimental arrangement was evidently somewhat akin to taking a photograph with the Sun behind the camera. A second factor influencing the level of the difference signal is the reflectivity of the targets, which, in our case, were perfect acoustic

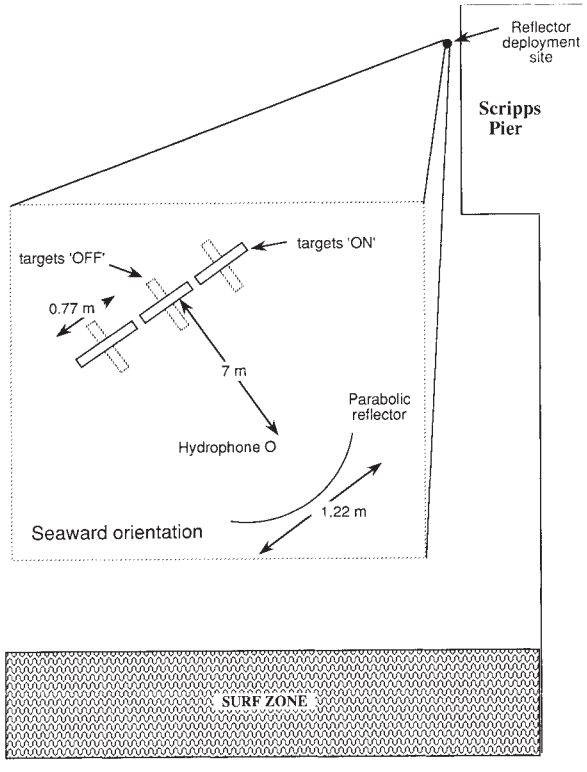

FIG. 2 Plan view of the seaward configuration of the parabolic reflector and targets off Scripps pier. The deployment site is ~200 m out from the shore. (Drawing not to scale).

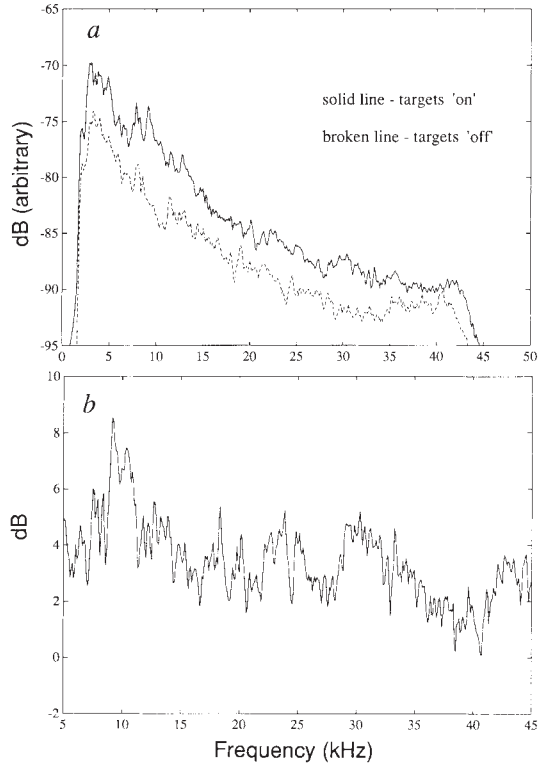

FIG. 3 *a*, Noise spectra obtained with the beam of the parabolic reflector orientated seaward and the targets at a range of 7 m. (The rapid roll-off above 43 kHz is an effect of anti-alias filtering.) *b*, Difference spectrum, illustrating the nominally uniform separation between the 'on' and 'off' spectra over most of the frequency band of interest.

reflectors; had they been absorbers of sound, they would have left a 'hole' in the noise field and the difference signal would have been zero or negative. A negative signal can form the basis of an image, a 'silhouette', the important criterion being that there should be an acoustic contrast between the object and its background.

Although this first acoustic daylight experiment in the ocean was successful, the observed spectrum is a far cry from a pictorial image on a television monitor. In effect, we have generated just one pixel of an image, corresponding to the single beam of the parabolic reflector. More pixels require more beams. These could be produced with a volumetric phased array, although other possibilities involving reflectors, either parabolic or spherical, and refractive acoustic lenses are also being considered. □

Received 6 November 1991; accepted 11 February 1992.

1. Urick, R. J. *Principles of Underwater Sound* (McGraw-Hill, New York, 1975).
2. Kerman, B. *Sea Surface Sound* (Kluwer, Dordrecht, 1988).
3. Melville, W. K., Loewen, M. R., Felizardo, F. C., Jessup, A. T. & Buckingham, M. J. *Nature* **336,** 54–56 (1988).
4. Mellen, R. H. *J. acoust. Soc. Am.* **24,** 478–480 (1952).
5. Buckingham, M. J. & Jones, S. A. S. *J. acoust. Soc. Am.* **81,** 938–946 (1987).
6. Glegg, S. A. L. & Buckingham, M. J. *Florida Atlantic Univ. Rep.* (July 1990).

ACKNOWLEDGEMENTS. We thank E. Slater and L. Green for the loan of the parabolic reflector and G. Deane for guidance on design of circuit elements. This work was supported by the Office of Naval Research.

Analytical model for solidification of the Earth's core

Bruce A. Buffett, Herbert E. Huppert, John R. Lister & Andrew W. Woods

Institute of Theoretical Geophysics, Department of Applied Mathematics and Theoretical Physics and Department of Earth Sciences, University of Cambridge, Cambridge CB3 9EW, UK

THE Earth's solid inner core is generally thought to have formed by gradual solidification of the liquid core as the Earth cooled[1–3]. To elucidate the relative importance of the various physical effects on the thermal evolution of the core, we have developed an analytical model based on global heat conservation, which describes the cooling of the vigorously convecting, fluid outer core and the concomitant growth of the inner core. We obtain a simple form for the evolution of the inner-core radius which allows the consequences of changes to the model's input parameters to be readily assessed. For most of this evolution, inner-core growth is controlled primarily by the heat capacity of the outer core and the history of the heat flux into the base of the mantle. Heat sources associated with solidification of the inner core, including the release of latent heat and gravitational energy, have a secondary role but become more important towards the end of solidification. Using current seismic estimates of compositional changes at the surface of the inner core, we conclude that the compositional and thermal buoyancy fluxes in the outer core are comparable.

The energetics of the cooling core have been studied previously[4–7] to estimate the energy available to power the geodynamo through the release of latent heat on solidification[8] and through the associated generation of compositional buoyancy[9] by the exclusion of light elements from the iron-rich inner core. Other studies[10–12] have attempted to construct thermal histories of the Earth's core using parameterized models of convection. The latter have all involved extensive numerical calculations, in contrast to the analytical model developed here.

In our model we assume that compositional and thermal buoyancy forces drive vigorous convection in the liquid outer core, and that the liquid core is well mixed with an adiabatic temperature profile. The potential temperature in the liquid core, which is defined as the temperature after subtracting the adiabatic variation, is therefore spatially uniform and slowly decreases with time (Fig. 1). We also assume that the surface of the inner core is in thermodynamic equilibrium with the surrounding liquid. With these two assumptions, the temperature through the outer core is uniquely determined by the solidification temperature, $T_s(p)$, which we treat as a function of pressure p only and hence implicitly of depth. The solidification temperature may also be a function of the slowly varying composition. At present, the details of the phase diagram for the iron alloy constituting the core are poorly constrained, but simple theoretical models suggest that the effect of compositional variations on T_s is small[7].

The heat extracted from the cooling outer core is transported through the overlying mantle to the surface of the Earth by thermal convection. Convective motions in the mantle[13] are characterized by effective viscosities of 10^{21}–10^{23} Pa s (refs 14–16). The cooling timescale associated with mantle convection is therefore much greater than that characteristic of convection in the outer core, where the viscosity is less than 5×10^{3} Pa s (ref. 17). Thus the relatively sluggish and more massive mantle controls the cooling of the core by regulating the heat flux $f_m(t)$ across the core–mantle boundary. The magnitude and time dependence of $f_m(t)$ will depend on the details of mantle convection, which include the distribution of radioactive isotopes and any compositional or rheological layering in the mantle. As many such details are unknown, we treat $f_m(t)$ as a prescribed parameter and focus on the evolution of the core. Different models of mantle convection will give rise to different values of $f_m(t)$, and these may be readily incorporated into our model.

The model is based on global heat conservation, which equates the heat lost from the core liquid plus the heat produced by growth of the inner core to the net heat flux from the outer core. The main sources of heat associated with the growth of the inner core are the latent heat released by solidification and the loss of gravitational energy due to the solidification of an iron-rich inner core. This gravitational energy is converted to heat by buoyancy-driven motions in the core. Further gravitational energy is released by adiabatic compression and thermal contraction of the Earth, but detailed numerical calculations (B.A.B., H.E.H., J.R.L. and A.W.W., manuscript in preparation) show that these additional effects are less important, and they are not considered further here. Radioactive heat sources in the core[18] could be explicitly included in the model, but such heat

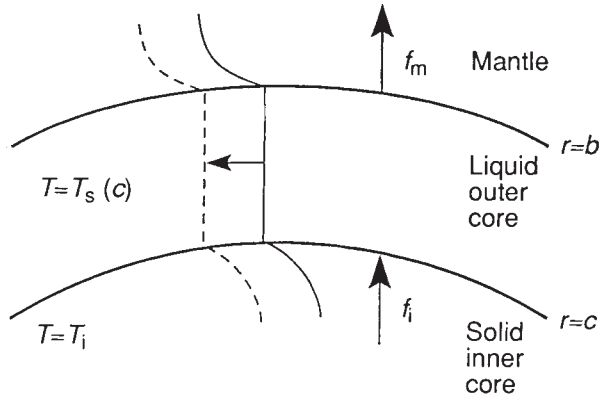

FIG. 1 Schematic profile of the potential temperature (the temperature after subtracting the adiabatic variation) in the slowly cooling core of the Earth. The solid line represents the temperature in the core and lower mantle at some instant. The dashed line represents the subsequent evolution of temperature as heat is continuously extracted from the core. Heat fluxes f_m and f_i pertain to the core–mantle and inner-core boundaries respectively. The solidification temperature $T_s(c)$ is defined at the inner core boundary, and $T_i(r, t)$ is the temperature within the inner core.